J. At. Mol. Sci.
doi: 10.4208/jams.022611.031311a

Vol. **2**, No. 4, pp. 294-304
November 2011

Elastic scattering of positron by gold atom

Kapil K. Sharma[a,*], Neerja[b], and R. P. Vats[a]

[a] *Department of Physics, M.S (P.G) College, Saharanpur (U.P), India*
[b] *Department of Electronics and Communication, A.B.E.S Engineering College, Ghaziabad (U.P), India*

Received 26 February 2011; Accepted (in revised version) 13 March 2011
Published Online 28 June 2011

Abstract. We present relativistic calculations of the differential, integrated elastic, momentum transfer total cross sections and spin polarization parameters for positrons scattered from Gold atom using a simple optical model potential to represent interaction between positron and target atoms in the energy range 2.0 – 500 eV. In the present calculation we employ a parameter-free model potential for the correlation polarization and absorption potential as devised for positron-atom scattering. The theoretical results are obtained from relativistic approach based on solving the Dirac equation using Hartree-Fock and Dirac-Fock wave functions.

PACS: 11.80.Fv

Key words: relativistic calculation, positron scattering

1 Introduction

In recent years positron-atom scattering has become a very interesting topic in both experimental and theoretical atomic collision studies [1–6]. As an alternative to electron-atom scattering, both the similarities and the differences between electrons and positrons mean that positron scattering provides a useful, and sometimes more sensitive, test of the techniques used to study the electron-scattering processes. This fact is particularly true from the standpoint of developing model interaction potentials for projectile-atom scattering. The similarities between electrons and positrons mass, magnitude of charge, and spin! Suggest that a consistent approach to devising model potentials should incorporate these quantities using similar logic for both projectiles. The differences between electrons and positrons, the sign of the charge, the possibility of positronium formation, and the fact that positron projectiles are distinguishable from the electrons of the target atom while electron projectiles are not offer important tests of how a model potential scheme handles issues such as projectile charge,

*Corresponding author. *Email address:* kapil81_physics@yahoo.co.in (K. K. Sharma)

inelastic thresholds, and correlations among projectile and target electrons. Therefore, model potentials that can reliably produce accurate scattering data for both electron- and positron-atom scattering signify an important step in our ability to perform these calculations quickly. These complications were so severe that it is only in last few years a few close-coupling types and many body calculations on lighter atoms like hydrogen, alkali and noble gas atoms have been attempted. The situation with respect to more complicated targets is less satisfactory. Besides the intrinsic importance of these methods, model potential approach and its variant also offer good opportunity to gain insight on the collision dynamics of the positron-atom scattering.

In the present paper, we use a parameter-free model optical potential to calculate the differential scattering cross section (DCS), spin polarization parameters, momentum and total cross sections. As a test case, we are presenting few results for e^+_ Au scattering. The present theory does not include the effect of Ps-formation. The relativistic Dirac equation is solved for both the elastic and total scattering of positrons from these atoms in the impact energy of 2.0 – 500.0 eV. The details can be found in our earlier paper [7].The optical potential $V(r)$ is represented as

$$V(r) = V_R(r) + iV_A(r), \tag{1}$$

where $V_R(r)$ refers to the real part of the projectile-target interaction. The use of only this part of the interaction yields pure elastic scattering. It consists of two parts: (i) Static potential V_S which is repulsive for the positron scattering and is obtained by averaging over the target wavefunction, (ii) a parameter-free correlation polarization potential (V_P). The inclusion of absorption potential $V_A(r)$ to the $V_R(r)$ in Eq. (1) gives the total scattering that includes both the elastic and inelastic scattering process, causing an absorption in a scattering beam. In most of the optical potential calculations as mentioned above, the correlation polarization potential and the absorption potential as devised for electron impact are often used for the positron case, although there is no justification for doing that. It is only recently a few attempts [3, 8] have been made to use the polarization and absorption of the target atom by positron impact in a more consistent manner. In the present study, we examine the effect of both, a true positron correlation potential (PCP) as given by Jain [9], a positron absorption potential (p Q V_a) as devised by Reid and Wadehra [3] and also by Sun *et al.* [17]. In the present paper to explore and test the further applicability of our optical potential approach we use the same method to study the elastic electron scattering from the ground state of Au atoms. The electronic configurations of their ground state are given in Table 1. In Section 2 we have briefly outlined our calculation while our results and discussions are presented in Section 3.

Table 1: Electronic configuration, term symbols, dipole polarizability, ionization potential (I.P), first excitation threshold E and crossing points (r_c) and for Au atoms.

Z (Atomic No.)	Element	Electronic configuration	Term	Polarizability (a.u)	I.P (eV)	E_{th} (eV)	Crossing point (a.u) (r_c)
79	Au	[Xe] 6s (2) 4f (14) 5d (10) 6s (1)	^{2}S	36.1	9.2255	2.4255	3.921

2 Theoretical calculation

2.1 Positron correlation polarization potential

The positron correlation polarization (PCP) potential is defined as a functional derivative of the corrective of the correlation energy with respect to $p(r)$, i.e.,

$$V_{\rm corr}(r)=\left(1-\frac{1}{3}r_s\frac{d}{dr_s}\right)\epsilon_{\rm corr}(r_s), \tag{2}$$

with r_s as a density parameter satisfying $4/3\pi r_s^3 p(r)=1$, where $p(r)$ is the target undistorted electronic density. Finally, an analytic expression is obtained (in atomic units) as

$$V_{\rm corr}=\begin{cases} (-1.82/\sqrt{r_s}+(0.051\ln r_s-0.115)\ln r_s+1.167)/2, & r_s<0.602, \\ \left(-0.92305-0.09098/r_s^2\right)/2, & 0.302\le r_s\le 0.56, \\ \left(-8.7674r_s(r_s+2.5)^{-3}+(-13.51+0.9552r_s)(r_s+2.5)^{-2}\right. & \\ \quad \left.+2.8655(r_s+2.5)^{-1}-0.6298\right)/2, & 0.56\le r_s\le 8.0. \end{cases} \tag{3}$$

We further mention that in the limit $r_s\to\infty$ the correlation polarization should approach the correct form of the polarization i.e., $V_{LR}=-\alpha_0/2r^4$. Thus, depending on the location of the projectile from the target, $V_{PCP}(r)$ for e^+-atom system is taken as

$$V_{PCP}(r)=\begin{cases} V_{\rm corr}(r), & r\le r_c, \\ V_{LR}(r), & r\ge r_c, \end{cases} \tag{4}$$

where r_c is the $V_{\rm corr}$ and V_{LR} cross each other for the first time.

2.2 Positron absorption potential

According to the quasi-free scattering approximation, the absorption potential for a projectile with local kinetic energy $E=p^2/2m$ passing through a free electron gas of density $p(r)$ is given by

$$V_{\rm abs}(r,E)=-\frac{1}{2}\rho(r)\overline{\sigma}(k_F,p)v_{\rm loc}, \tag{5}$$

where $v_{\rm loc}=[2(E-V_R(r))/m]^{1/2}$ is the local velocity of the projectile for $(E-V_R)\ge 0$ and $k_F=[3\pi^2\rho(r)]^{1/3}$ is the Fermi momentum. The $\overline{\sigma}(k_F,p)$, the average quasi-free binary collision cross section, is given as

$$\overline{\sigma}_b=\frac{1}{p}\int N(k_F,q)\left|\vec{p}-\vec{q}\right|d\vec{q}\int\frac{d\sigma_b}{d\Omega}\left(\frac{1}{p_0^2}\delta(p_0-p_f)\Theta(q',k_F)\right)d\vec{g}, \tag{6}$$

where, $\vec{p}(\vec{p}')$ and $\vec{q}(\vec{q}')$ are the laboratory frame momenta of the incident positron and target electron, respectively before and after the collision. The vectors $\vec{p}_0$ and $\vec{p}_f$ are the initial and

final momenta of the positron in center-of-mass frame of the binary system. The function $N(k_F,q)$ refers to the target electron momentum distribution given as

$$N(k_F,q)=\begin{cases} N(k_F), & q\le k_F, \\ 0, & q>k_F, \end{cases} \tag{7}$$

where $N(k_F)=3/(4\pi k_F^3)$. The momentum transfer vector $\vec{g}$, is given as $\vec{g}=\vec{p}'-\vec{p}=\vec{q}-\vec{q}'$. The $d\sigma_b/d\Omega$ is the differential binary cross section based on Rutherford scattering as

$$\frac{d\sigma_b}{d\Omega}=\frac{2}{g^4}. \tag{8}$$

The function $\Theta(\vec{q}',k_F)$ in Eq. (3.8) is unity for Pauli allowed final states of the binary collision and zero for Pauli blocked final states in the binary collision. For positron quasi-free scattering this function become

$$\Theta(q',k_F)=H(q'^2-k_F-\omega), \tag{9}$$

where $\omega=2\Delta$, with Δ being the energy gap between the target ground-state energy and the final energy of the originally bound target electron and $H(q'^2-{k_F}^2-\omega)$ is the Heaviside unit step function, which equals to one when the argument is non-negative and zero otherwise. The average binary collision cross section $\overline{\sigma}_b$ can be expressed as

$$\overline{\sigma}_b(k_F,p)=\frac{16\pi^2}{p^2}N(k_F) \times\begin{cases} \frac{4}{3}\frac{k_F^3}{\omega}+4k_F+2p\ln\left|\frac{p-k_F}{p+k_F}\right|, & p^2-\omega\ge k_F^2, \\ \frac{4}{3}\frac{(p^2-\omega^2)^{3/2}}{\omega}+4(p^2-\omega)^{1/2}+2p\ln\left|\frac{p-\sqrt{p^2-\omega}}{p+\sqrt{p^2-\omega}}\right|, & k_F^2\ge p^2-\omega\ge 0. \end{cases} \tag{10}$$

3 Results and discussion

We have performed two types of calculations using a complex optical potential: one without absorption potential, i.e., taking only a real optical potential, and another with an absorption potential. These two calculations are referred to as SP and SPA respectively. Thus, our SP calculation includes static and polarization potentials in the optical potential and is real, while the SPA calculation has in addition an absorption potential in the optical potential and is a complex quantity. We present our results for e^+-Au mainly at energies up to 2.0 to 500 eV.

3.1 Differential cross section and asymmetry parameter

We first present in Fig. 1(a)–(f) our SP and SPA calculations for the differential cross sections and the asymmetry parameter S, T and U for the elastic scattering of positrons from the

Au atom at various energies 5, 10, 50, 100, 200 and 500 eV. From the DCS results it can be seen that the present theory predicts the sharp forward and backward peaks, associated with a number minima and maxima in between. As seen the SPA calculations show that the absorption potential reduces the DCS. Further, the structure of dips and humps is broad for e^+-Au scattering. We find that the rapid variation of S with scattering angles is much different for our SP and SPA calculations. The shape of curves goes on changing as we go from low to higher energies. We hope that new experimental results will be reported in the light of our calculation for the elastic e^+- Au scattering.

3.2 Angle-integrated elastic cross sections and contribution of partial waves

The present results for various cross sections are shown for the positron energy range; 0 – 10 eV. This is the range in which the present results are expected to be most accurate because for the cases gold atoms the range $E > 5$ eV is beyond the energy region in which positronium formation is its most important. The maximum in the d-wave cross-sections arises from shape resonance at energies $E_r \approx 2.5$ eV for e^+-Au scattering respectively. The total cross-sections are also plotted in the figure under this model. Each curve shows a narrow low-energy peak

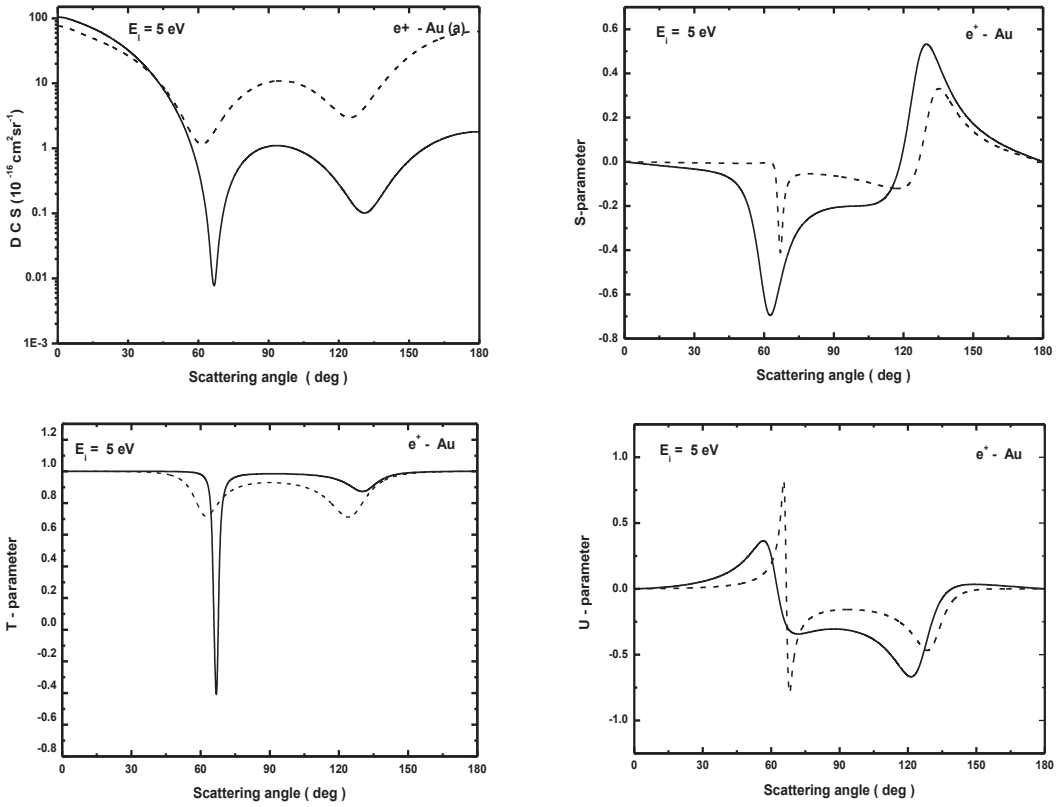

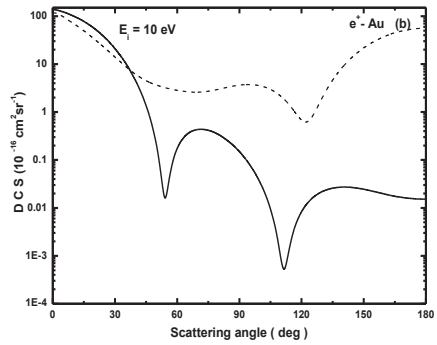
E_i = 10 eV
e+ - Au (b)
D C S (10 -16 cm2 sr-1)
Scattering angle (deg)

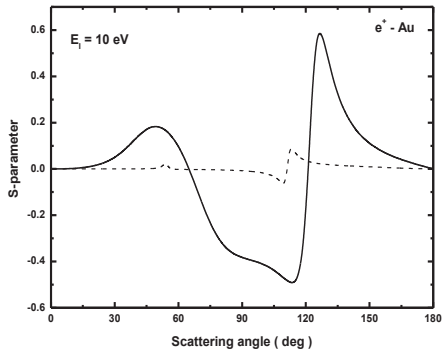
E_i = 10 eV
e+ - Au
S-parameter
Scattering angle (deg)

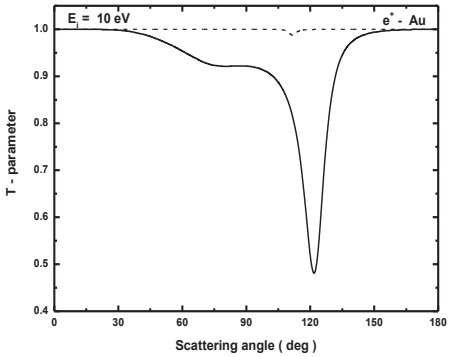
E_i = 10 eV
e+ - Au
T - parameter
Scattering angle (deg)

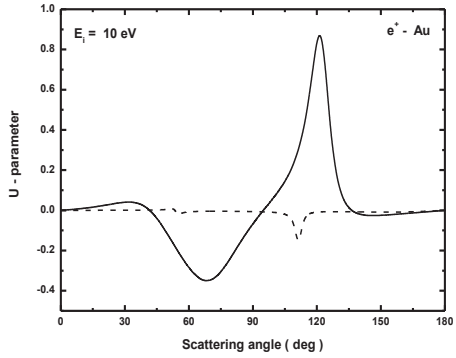
E_i = 10 eV
e+ - Au
U - parameter
Scattering angle (deg)

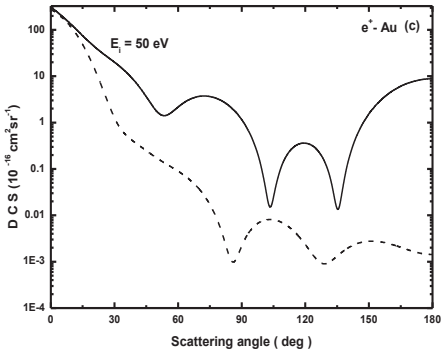
E_i = 50 eV
e+ - Au (c)
D C S (10 -16 cm2 sr-1)
Scattering angle (deg)

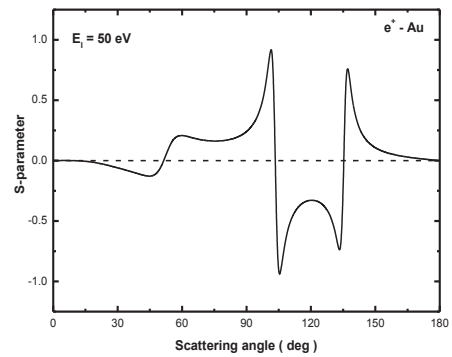
E_i = 50 eV
e+ - Au
S-parameter
Scattering angle (deg)

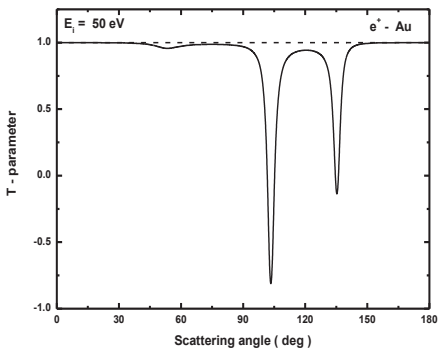
E_i = 50 eV
e+ - Au
T - parameter
Scattering angle (deg)

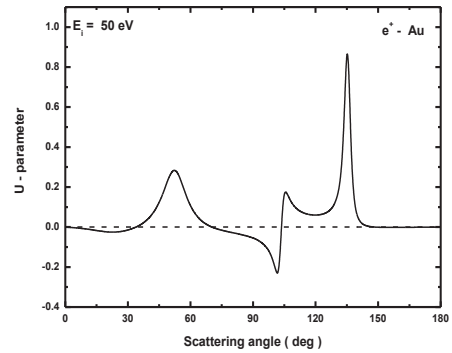
E_i = 50 eV
e+ - Au
U - parameter
Scattering angle (deg)

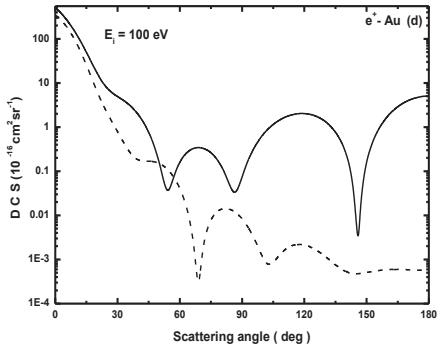
e+ - Au (d)
Ei = 100 eV
D C S (10-16 cm2sr-1)
Scattering angle (deg)

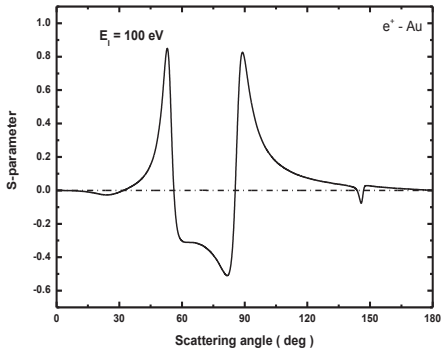
Ei = 100 eV
e+ - Au
S-parameter
Scattering angle (deg)

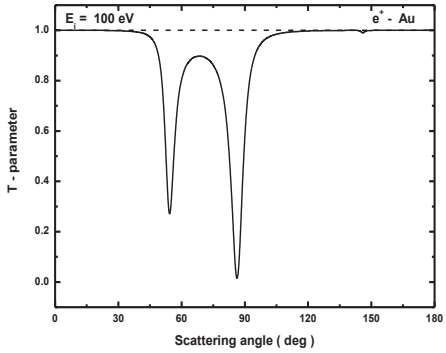
Ei = 100 eV
e+ - Au
T - parameter
Scattering angle (deg)

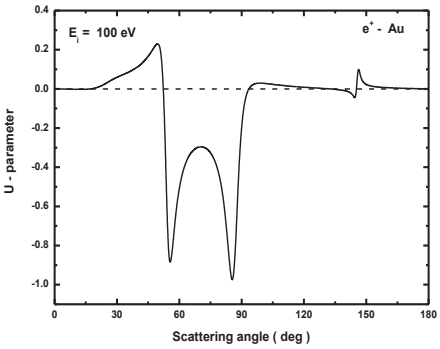
Ei = 100 eV
e+ - Au
U - parameter
Scattering angle (deg)

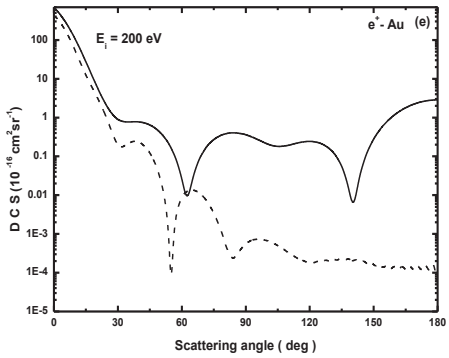
e+ - Au (e)
Ei = 200 eV
D C S (10-16 cm2sr-1)
Scattering angle (deg)

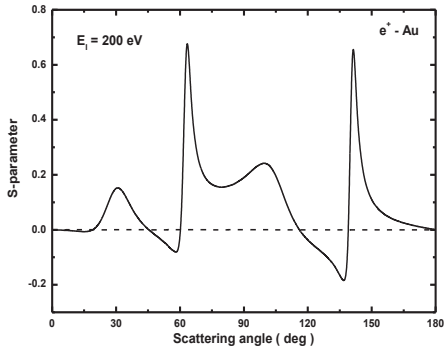
Ei = 200 eV
e+ - Au
S-parameter
Scattering angle (deg)

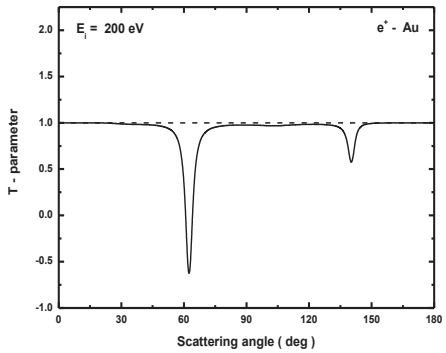
Ei = 200 eV
e+ - Au
T - parameter
Scattering angle (deg)

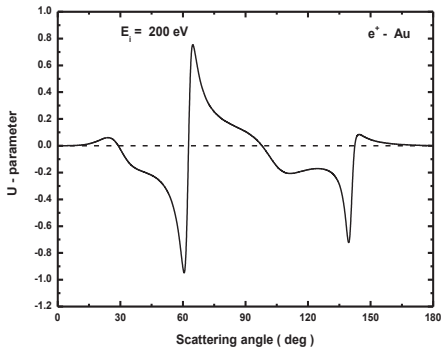
Ei = 200 eV
e+ - Au
U - parameter
Scattering angle (deg)

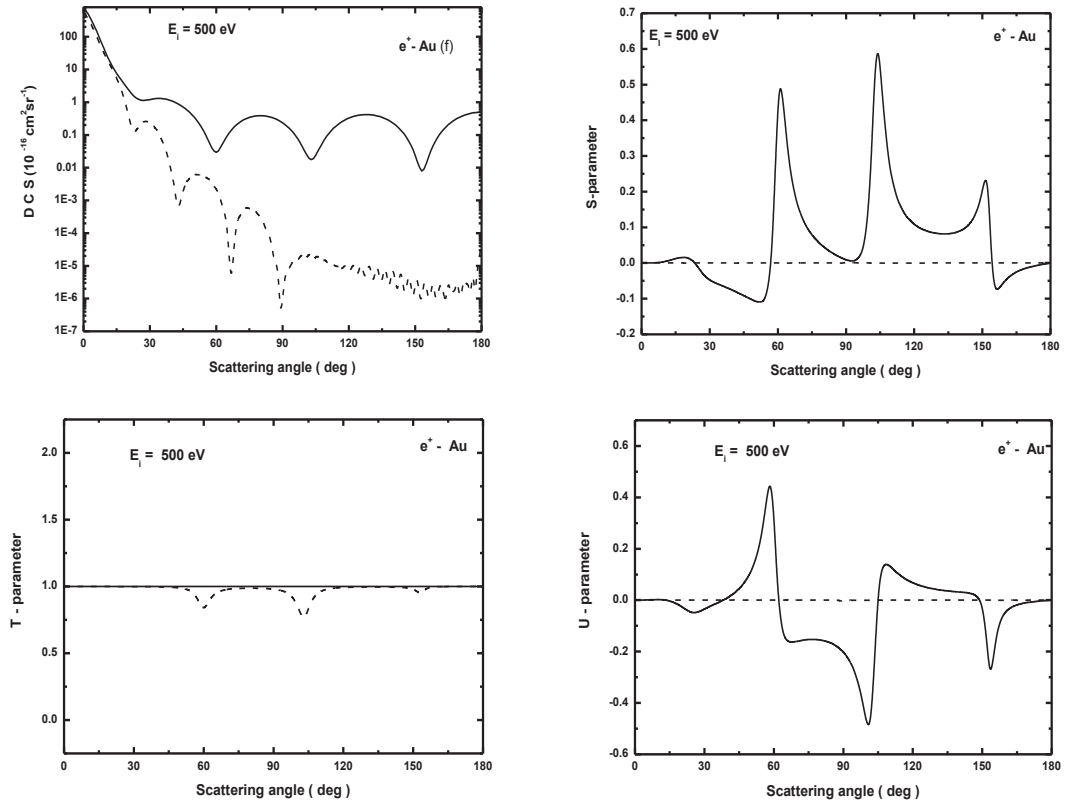

Figure 1: Elastic e^+ - Au scattering: DCS at energies (a) 5 eV, (b) 10 eV, (c) 50 eV, (d) 100 eV, (e) 200 eV, (f) 500 eV and the asymmetry parameter S, T and U at same energies. Present calculation: —— with complex potential (SPA); - - - - with real potential (SP).

followed by sharp fall of the cross-sections up to the first inelastic threshold. It is observed from Fig. 2 that first inelastic threshold energy E_{th}, p and d wave partial cross-sections contributes maximum to σ_{el} and near and above to E_{th}, f wave dominates. Calculations were least accurate in the energy region near and below the peak in the positronium formation cross sections.

3.3 Elastic, total and momentum-transfer cross sections

The results of our present integrated elastic, total and momentum-transfer cross sections for Au atoms are presented in Tables 2 and 3. The elastic cross sections are obtained using both the real and complex potentials. It is noted that at all energies the elastic cross sections obtained with only real potential are larger than those obtained with the complex potential, i.e., This is not unexpected as we have seen that the inclusion of absorption reduces the DCS and consequently, the angle-integrated cross section. The total cross section descends rapidly

at lower energies and thereafter varies slowly with increasing impact energies. We find that

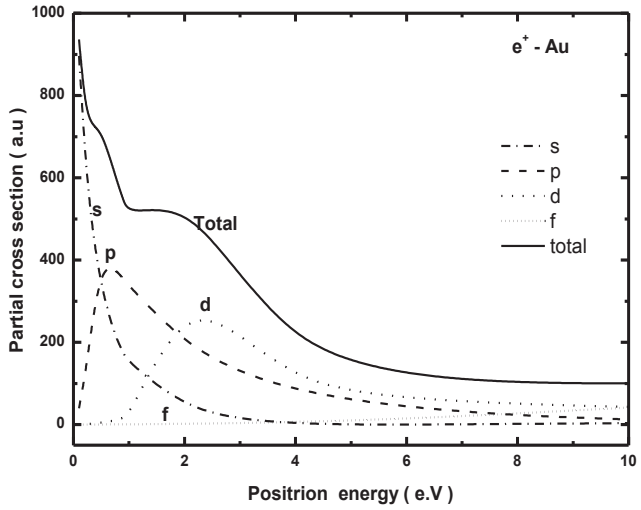

Figure 2: Partial cross-sections in unit of 10^{-16} cm^2 for scattering of e^+ - Au. Present calculation s, p, d, and f waves, and summed integral cross section.

Table 2: Elastic (σ_{el}), absorption (σ_{abs}), and total (σ_t) cross-sections in units of 10^{-16} cm^2 for Au in σ_{el} SPA with absorption effect. σ'_{el} is the elastic scattering cross section without absorption effect SP.

Energy (eV)	σ^+-Au			
	σ'_{el}	σ_{el}	σ_{abs}	σ_t
2.0	538.325	538.325	0	538.325
5.0	154.841	76.2318	117.11	193.342
10.0	106.949	58.422	100.652	159.074
15.0	112.015	45.4989	81.1775	126.676
20.0	101.483	39.3133	69.9972	109.31
30.0	78.6809	32.5796	56.73	89.3166
50.0	56.1403	27.2705	45.8435	73.114
80.0	51.7589	25.0006	41.2106	66.2112
100.0	43.7782	21.2366	33.7412	54.9778
150.0	37.4991	18.826	29.1777	48.0037
200.0	32.8488	17.0975	26.0375	43.1351
250.0	29.3578	15.7746	23.7138	39.4884
300.0	26.688	14.7172	21.9074	36.6245
350.0	24.5843	13.8451	20.4522	34.2973
400.0	22.8732	13.1086	19.2482	32.3569
450.0	21.5052	12.475	18.2309	30.7059
500.0	538.325	538.325	16.3456	538.325

Table 3: Momentum transfer cross-section (σ_m) in units of 10^{-16} cm^2 for e^+-Au Scattering.

Energy (eV)	σ^+-Au	
	SP	SPA
2.0	256.256	256.256
5.0	83.1397	27.7904
10.0	45.6652	14.1809
15.0	56.7713	7.34845
20.0	44.4176	5.0964
30.0	26.326	3.31013
50.0	15.6587	2.27591
80.0	11.2035	1.90518
100.0	5.92559	1.36211
150.0	4.432	1.05661
200.0	4.04777	0.858134
250.0	3.93831	0.71898
300.0	3.86107	0.61647
350.0	3.74761	0.538079
400.0	3.5958	0.476296
450.0	3.42102	0.426393
500.0	256.256	256.256

our values are in good agreement with them.

4 Conclusion

We have presented our calculations using a relativistic optical potential approach for the elastic scattering of positron from the heavier Gold atom. We have reported differential cross section and angular variation of the spin polarization parameters S, T, U as well as angle integrated elastic, total and momentum-transfer cross sections. The results are obtained in the two models, namely SP and SPA. It would be interesting to have more experimental measurements of the DCS and asymmetry parameters new results for e^+ - Au scattering to test our model potential approach at all energies and in the wide range of scattering angles. This will further enable one to construct a better choice of optical potential as compared to the present optical model we have used.

References

[1] T. S. Stein, J. Jiang, W. E. Kauppila, *et al.*, Can. J. Phys. 74 (1996) 313.
[2] M. W. J. Bromley, J. Mitroy, and G. Ryzhikh, J. Phys. B: At. Mol. Opt. Phys. 31 (1998) 4449.
[3] D. D. Reid and J. M. Wadehra, J. Phys. B: At. Mol. Opt. Phys. 29 (1996) L127; Phys. Rev. A 57 (1998) 2583.
[4] M. T. McAlinder, A. A. Kernoghan, and H. R. J. Walters, J. Phys. B: At. Mol. Opt. Phys. 30 (1997) 1543.

[5] G. F. Gribakin and J. W. A. King, Can. J. Phys. 74 (1996) 449.
[6] M. Basu, M. Mukherjec, and A. S. Ghosh, Phys. Rev. A 43 (1991) 4746.
[7] Neerja, A. N.Tripathi, and A. K. Jain, Phys. Rev. A 61 (2000) 032713.
[8] S. N. Nahar and J. M. Wadehra, Phys. Rev. A 35 (1987) 2051.
[9] A. K. Jain, Phys. Rev. A 41 (1990) 2437.
[10] A. D. McLean and R. S. McLean, At. Data Nucl. Data Tables 26 (1981) 197.
[11] F. Salvat, J. D. Martinez, R. Ayol, and J. Parellada, Phys. Rev. A 36 (1987) 467.
[12] W. E. Kauppila, C. K. Kwan, D. Przybyla, *et al.*, Can. J. Phys. 74 (1996) 474.
[13] D. F. Registar, L. Vuskovic, and S. Trajmar, J. Phys. B: At. Mol. Phys.19 (1986) 1685.
[14] R. P. McEachran, A. D. Stauffer, and L. E. M. Campbe, J. Phys. B: At. Mol. Phys. 13 (1980) 1281.
[15] H. Mohan, A. K. Jain, and S. Sharma, J. Phys.: Conf. Ser. 199 (2010) 012023.
[16] R. K. Gangwar, A. N. Tripathi, L. Sharma, and R. Srivastava, J. Phys. B: At. Mol. Opt. Phys. 43 (2010) 085205.
[17] J. Sun, G. Yu, Y. Jiang, and S. Z hang, Eur. Phys. J. D 4 (1998) 83.